



Suspect and non-target screening of per- and polyfluoroalkyl substances (PFAS) and other halogenated substances in electrochemically oxidized landfill leachate and groundwater

Svante Rehnstam^a, Sanne J. Smith^{a,b}, Lutz Ahrens^a

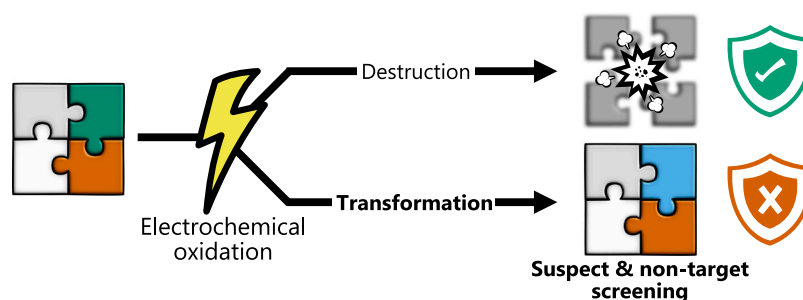
^a Swedish University of Agricultural Sciences (SLU), Department of Aquatic Sciences and Assessment, Lennart Hjelm's väg 9, 756 51 Uppsala, Sweden

^b Delft University of Technology, Department of Water Management, Stevinweg 1, 2628 CN Delft, the Netherlands

HIGHLIGHTS

- EO as destructive treatment for PFAS-contaminated landfill leachate and groundwater.
- Identification of new halogenated substances using suspect and non-target screening.
- Transformation products identified originating from electrochemical process.
- New pathways identified for transformation of PFAS.

GRAPHICAL ABSTRACT



ARTICLE INFO

Keywords:

Per- and polyfluoroalkyl substances
High-resolution mass spectrometry
Electrochemical oxidation
Non-target screening
Destructive treatment
Transformation products

ABSTRACT

Release of persistent and potentially toxic per- and polyfluoroalkyl substances (PFAS) and other halogenated compounds into the aqueous environment is an emerging issue and advanced treatment methods are needed for their removal from contaminated water. Destructive treatment methods for PFAS exist, but there is a risk of incomplete degradation, resulting in creation of transformation products during treatment. This study assessed the potential of electrochemical oxidation (EO) for destruction of PFAS and other halogenated compounds, and their transformation products. Suspect and non-target screening were used to explore the chemical space of these samples and identify compounds present before and after the treatment, including transformation products. In total, 21 PFAS classes and 53 individual PFAS were identified using suspect and non-target screening, with confidence level (CL) 3d or higher. Two new classes of PFAS (FASHN and MeOH-FASA) were discovered for the first time. Suspect screening of PFAS revealed that hydro-substituted and ether PFAS could be formed during EO. A total of 12 chlorinated and two brominated compounds were also detected and confirmed with CL 1–3, with six compounds determined to be transformation products. Formation of ammonium oxidation byproducts was hypothesized as being responsible for most identified transformation products formed during EO.

E-mail address: svante.rehnstam@slu.se (S. Rehnstam).

<https://doi.org/10.1016/j.jhazmat.2024.136316>

Received 23 May 2024; Received in revised form 7 October 2024; Accepted 25 October 2024

Available online 28 October 2024

0304-3894/© 2024 The Authors. Published by Elsevier B.V. This is an open access article under the CC BY license (<http://creativecommons.org/licenses/by/4.0/>).

1. Introduction

Landfills are often considered point sources of environmental contamination [1]. Organic micropollutants in landfill leachate can have adverse effects on nearby soil, groundwater, and surface water ecosystems [2,3]. Efforts are taken to reduce the environmental impact from landfill facilities, e.g., conventional wastewater treatment techniques such as aerobic and anaerobic biological processes, chemical oxidation, and chemical precipitation are commonly utilized at such sites [4]. More advanced treatment techniques involving e.g., granular activated carbon (GAC) are sometimes included to remove organic micropollutants [5].

Per- and polyfluoroalkyl substances (PFAS), a group of halogenated organic micropollutants, are difficult to remove or degrade in water treatment processes [6]. These compounds are known for being extremely chemically and thermally persistent, potentially bio-accumulative, and toxic [7]. Due to their unique characteristics, they are widely used in products such as textiles, aqueous film-forming foams (AFFF), and non-stick coatings [8]. The most common technology for removing PFAS from water matrices is through adsorption to GAC, where PFAS are bound to a sorbent but not destroyed [9]. This creates a separate waste stream, which has to be taken care of [10]. Destructive treatment methods are typically not cost-efficient, due to the high energy intensity required to break down PFAS [11]. Combinations of different treatment methods to concentrate the waste stream and then destroy the concentrated waste have advantages over individual advanced treatment processes [12]. One example is combined foam fractionation as a concentration treatment and electrochemical oxidation (EO) as a destructive treatment [13,14].

Foam fractionation relies on the surfactant properties of many PFAS, particularly perfluoroalkyl acids (PFAA), adsorbing these compounds on rising air bubbles [15]. Presence of sufficient amphiphilic substances in water leads to formation of a foam in which PFAS are enriched. Removing this PFAS-rich foam from the water surface results in a relatively PFAS-free effluent. The PFAS in the foam fraction can be destroyed by e.g., EO, which uses anodic materials with high overpotential for the oxygen evolution reaction [16]. Direct electron transfer to the anode is the first step in oxidation of PFAS, after which the perfluoroalkyl chain is generally assumed to 'unzip', ideally ultimately achieving full defluorination. However, formation of transformation products, including PFAS, is a well-known issue [17,18].

Formation of transformation products is an unwanted process in most degradation processes, because complete PFAS mineralization is the ultimate goal [12,18]. The transformation products that may form during the EO process have not been widely investigated, since most studies rely on quantification of PFAS concentrations using targeted triple-quadrupole mass spectrometer techniques [18,19]. Advanced oxidation processes may also result in formation of harmful chlorinated and brominated transformation byproducts [13]. There is thus an urgent need for untargeted analyses to investigate how halogenated substances are (trans)formed during the EO process, to assess formation of possibly harmful degradation (by)products. Untargeted analyses are particularly important for complex matrices such as landfill leachate, because the presence of co-contaminants results in an even wider range of possible degradation (by)products.

Suspect screening and non-target screening (NTS) are analytical techniques appropriate for identifying compounds and molecules when authentic standards and surrogates are not available [20]. Suspect screening relies on databases and previously recorded data, while NTS relies instead on feature prioritization [21]. In suspect screening, efforts are made to expand the scope beyond what has already been detected, to predict transformation products through chemical transformation simulation [22]. There have also been advances in NTS specifically for PFAS, most notably the software FluoroMatch developed by Koelmel and co-workers to streamline the NTS workflow [23–25].

A previous study by our research group [13] showed that EO with

boron-doped diamond anodes can successfully degrade PFAS in landfill leachate and groundwater, with or without foam fractionation as a pre-treatment step. Additional analyses performed as part of that study, most notably effect-based bioassays and extractable organofluorine (EOF) analyses, indicated the presence of unknown fluorinated and potentially toxic compounds. Those findings prompted the present study, which aimed to identify transformation products formed during EO by utilizing untargeted techniques with high-resolution mass spectrometry coupled to liquid chromatography (LC-HRMS).

2. Experimental

2.1. Samples

Four different water types were treated electrochemically: (i) groundwater and (ii) landfill leachate from a landfill facility located in Uppsala, Sweden, and foam from (iii) groundwater and (iv) landfill leachate treated using foam fractionation from our previous study [26]. For all four water types, samples representing 0 h (initial water) and 1, 3, 5, 7, and 9 h ($t = 0-9$) of EO treatment were analyzed. The foam fractionation setup used a 10 cm diameter column, into which a peristaltic pump was pumping groundwater and leachate water. The foam generated from the air introduced through the air inlet was collected in foam collection vessels. Electrochemical oxidation was performed with a feed tank and a 20 L flow-through cell which was equipped with a boron-doped diamond anode and stainless steel cathode. For details of the experimental set-up and sample extraction, see [13].

2.2. Instrumental analysis

Liquid chromatography (LC) was performed using a Vanquish Horizon UPLC system. It was coupled to a QExactive Focus Orbitrap mass spectrometer (Thermo Fisher Scientific, Bremen, Germany), with a heated electrospray ionization source (HESI-II) run in negative ionization mode. Samples (10 μ L) were injected using a LC TriPlus RSH autosampler. The chromatographic system used a gradient mobile phase program consisting of an aqueous solvent with 5 mM of ammonium acetate and an organic solvent with 5 mM ammonium acetate, all run with a flow rate of 0.3 mL min⁻¹. For details of the gradient program, see Table S1 in Supplementary Information (SI). The Orbitrap was run in negative polarity mode, set to perform a full scan over the range 100–1000 m/z . For collection of MS² data, the instrument used data-dependent acquisition (DDA) in *discovery mode* (loop count set to $n = 3$). The ion source settings were as follows: sheath gas flow rate 45 a.u., auxiliary gas flow rate 10 a.u., sweep gas flow rate 0 a.u., spray voltage 4.1 kV, capillary temperature 350 °C, S-lens RF level 25 a.u., and auxiliary gas heater temperature 400 °C.

2.3. Data processing

The raw data obtained in LC-HRMS were processed using Compound Discoverer (version 3.3), in two separate tailored modular workflows (for details, see Table S2 in SI). One workflow was tailored for PFAS analysis and the other for compounds containing bromine and chlorine. For a peak to be considered a feature, it needed to have signal to noise ratio (S/N) greater than 3 and signal intensity greater than 10,000 counts. The use of a low S/N is to avoid false negatives (type II errors) in the early stages of processing, which is common practice in untargeted analyses [20,27]. The PFAS plugin from ThermoFisher [28], which is based on the work of Kaufmann et al. [29] and Koelmel et al. [24], was used to determine mass over carbon (m/C) and mass defect over carbon (md/C) ratios, for initial screening of potential peaks [29,24,25]. The plugin also contained a list of known PFAS fragments recorded in MS/MS measurements.

For PFAS, peak picking resulted in a total number of 144,387 features being detected (Fig. 1). Blank subtraction was performed to

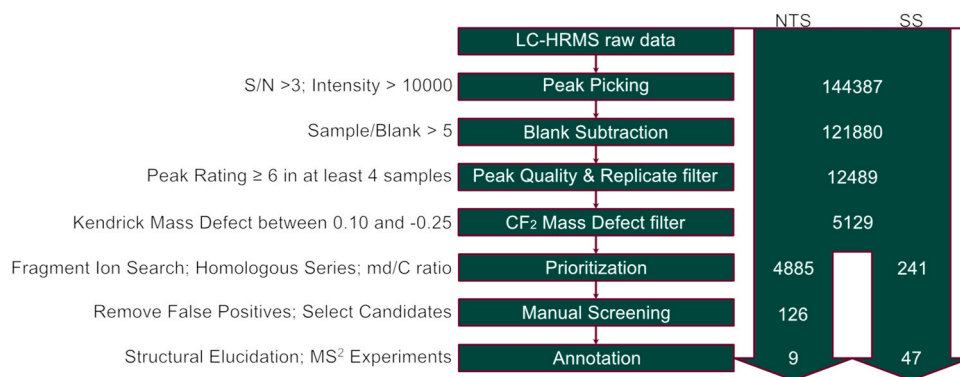


Fig. 1. Flow chart summarizing the non-target (NTS) and suspect screening (SS) process.

remove any contaminants introduced from sample preparation and laboratory equipment, which reduced the number of features to 121,880. After blank subtraction, quality control of the detected features was performed by utilizing the peak rating algorithm in Compound Discoverer, where a peak need to be present in all four replicates and have a peak rating greater than 6 to be considered a real feature, resulting in a total of 12,489 features. Peak rating is calculated based on four main factors, namely full-width half maxima to base (FWHM2Base), Jaggedness, Modality, and Zig-Zag. FWHM2Base is calculated based on a ratio of the peak width at half height divided by the peak. The peak rating is reversely proportional to the value of FWHM2Base. Jaggedness measures how many times the intensity of a peak alternate between going up and down in a row, where a low Jaggedness value will result in a higher peak rating. Modality will look for unexpected valleys in a peak that may occur before reaching baseline. Once again a low value for Modality will increase the peak rating. The final factor, Zig-Zag, calculates the mean number of valleys in one peak and divide it by the peak height from baseline. A high Zig-Zag value will result in a low peak rating. For more details on how the peak rating calculations are performed see the Compound Discoverer User Guide for LC Studies [30]. Details of data processing are provided in Table S2 in SI.

For brominated and chlorinated compounds, peak picking resulted in 146,007 features, which were reduced through blank subtraction (123,280 features) and peak quality and replicate filter (12,711 features) (Fig. S1 in SI).

2.4. Suspect screening for identification of PFAS

After peak rating, all peaks which did not fall within a CF₂-adjusted Kendrick mass defect (KMD) of -0.25 and 0.10 were filtered out, which resulted in 5129 final features, although this step was only performed in the PFAS analysis (Fig. 1). Suspect screening for PFAS was performed using a suspect list obtained from the NORMAN Network's substance database, which was filtered for PFAS [31] ($n = 1291$), Chemical List PFASSTRUCT-2022-04-20 ($n = 10737$) and PFAS_NIST obtained from the ThermoFisher PFAS plugin ($n = 4951$) [28], and the *in-silico* generated suspect list ($n = 36604$) from Getzinger et al. [22] (in total $n = 53,643$, with compound overlapping between the suspect lists) [22]. Prioritization was performed using the suspect screening lists by filtering out all features without a hit, which resulted in 241 features. After further manual annotation, mainly to remove false positives, 44 features were identified.

2.5. Suspect screening for identification of brominated and chlorinated compounds

For brominated and chlorinated compounds, only the NORMAN Network's substance database was used [32]. The database was first filtered to include only drinking water chemicals and then further

filtered for disinfection by-products. Finally, one suspect list for chlorinated compounds was made by filtering for compounds containing "Cl" ($n = 6313$) and one was made for brominated compounds by filtering for compounds containing "Br" ($n = 1909$) (Fig. S1 in SI).

All compounds with hits from ChemSpider or the suspect lists were subjected to the fragment ion search (FISH) function in Compound Discoverer. This feature created *in-silico* fragments of the proposed structures and produced a match factor based on the number of peaks from the MS² data that matched the *in-silico* generated fragments. The proposed structures were ranked and prioritized based on the number of matching FISH fragments. Compounds which had a FISH score higher than zero were controlled for false positives (23 features) and then further manually annotated (14 features).

2.6. Non-target screening for identification of PFAS

Non-targeted screening comprised four parts: (i) iterative-DDA using the IE-Omics R script developed by Koelmel et al. (2017); (ii) fragment flagging, which is referred to as 'compound classes' in Compound Discoverer; (iii) a mass defect vs carbon number approach, as described by Kaufmann et al. [29]; and (iv) homologous series identification, which was performed by an in-house written R-script [33].

The iterative-DDA strategy was developed to generate as many MS² spectra as possible in the shortest possible time (Koelmel et al., 2017). Using iterative DDA made other strategies such as fragment flagging more powerful, as they depend on the presence of MS² data.

The mass defect vs carbon number approach was used as a first step in feature prioritization [29]. Features with m/C ratio greater than 35 and less than -0.0007 were investigated. When all fragment ion search potential hits, homologous series hits, and md/C ratio hits were combined, a total of 4885 features was obtained. These features were further categorized manually as false positives or potential hits, resulting in a final total of 126 features, which were then further annotated. The final total of nine annotated compounds was obtained from non-target screening.

Fragment flagging was enabled by integration of the FluoroMatch fragment library into Compound Discoverer. The fragment library contained over 800 curated diagnostic fragments, which were used as prioritization tools. If a feature which contained MS² data had a fragment that matched any fragment in the library, it was given a Compound Class Score greater than zero. The feature list was then sorted in terms of abundance of fragments matching the library, and false positives and potential hits were categorized.

In homologous series identification, the final prioritization strategy used in non-target screening, the feature list was first curated based on quality control from peak ratings and no false positives from previous investigations. Features that remained were exported to an Excel file, which was then imported into R and subjected to the in-house R script for identifying homologous series. The homologous series scripts can be

found on GitHub [33].

For both suspect and non-target screening results, confidence level (CL) was determined based on a modified version, where the modifications were adjusted to better reflect CL in PFAS [34,35].

2.7. Quality control

Quality control was performed before and after the instrumental analysis. The mass spectrometer was first calibrated with the standard Pierce Mix for negative mode calibration on an QExactive Focus Orbitrap and then a mixture of chemicals was injected five times into the instrument with a fast gradient. The mass accuracy of the injected standards was determined, and in all cases fell well within the 3 ppm limit set in the laboratory. After analysis, the mass accuracy was once again measured by injecting the standard mixture five more times. If the value fell within the 3 ppm limit, the quality of the analysis was deemed acceptable.

2.8. Numerical data analysis

The Compound Discoverer software used for feature detection and evaluation also calculates the average area of each feature in every sample matrix and time point based on the median value. These median values were used to calculate the relative area of each compound of interest to evaluate how they were affected by the water treatment process.

The data were processed in R, using the *tidyverse* and *stringr* packages for data wrangling and creating graphics [36–38]. Relative areas for compounds and features obtained from Compound Discoverer were first processed by normalizing all values, that meaning both PFAS results and Br & Cl results, to the area of an internal standard present in all samples (¹³C₈-PFOA internal standard (IS)). Each compound featured in any of the heatmap plots had its area normalized as a percentage total area summed. The relative area was then plotted as a color, with the time point with the greatest area given the darkest hue.

3. Results and discussion

3.1. Suspect screening of PFAS

In total, 17 PFAS classes and 47 individual PFAS were identified using suspect screening at CL 1–3 in treated and untreated samples (Table 1). Five individual PFAS (perfluorononane sulfonic acid, perfluoroundecanoic acid, perfluorododecanoic acid, perfluorotridecanoic acid, and perfluorotetradecanoic acid) identified in concentrations close to the limit of quantitation using the targeted method in our original study [13] were not identified here.

All perfluoroalkyl carboxylic acids (PFCA, ID 1 f) and all perfluoroalkyl sulfonic acids (PFSA, ID 2 f) except perfluoropropane sulfonic acid (PFPrS) were identified at CL 1a and confirmed with reference standards. PFPrS was identified at CL 2a, due to co-occurrence of many homologues with higher retention times and similar fragmentation patterns in the MS² data. The fragments observed in the MS² data matched other PFSA. PFPrS was the only PFAA detected here that was not included in the targeted method developed in our previous study [13].

Three fluorotelomer sulfonates, 4:2 FTSA, 6:2 FTSA, and 8:2 FTSA, were detected and confirmed at CL 1a. Three cyclic PFSA were identified (ID 4 f, 5 f, and 6 f), of which perfluoroethylcyclohexane sulfonic acid (PFECHS, level 1a) was the only one confirmed with a standard. Additionally, two isomers of PFECHS were present, but they could only be determined at CL 3a, due to uncertainty of the position of the perfluorinated ethyl group. Two homologues of PFECHS with identical fragmentation patterns were also detected. These were perfluoromethylcyclohexane sulfonic acid (PFMCHS) and perfluorocyclohexane sulfonic acid, which were identified at CL 3a and 2b,

respectively. Cyclic PFSA have been detected previously in various environmental matrices, such as lakes and other surface water bodies [39]. We also want to acknowledge the difficulty with differentiating cyclic PFAS and unsaturated linear PFAS, but we do believe in this work that these were indeed cyclic in structure [34].

Perfluoroalkyl sulfonamides (FASA, ID 7 f) were detected with chain length of C_{3–6}, in addition to the previously quantified C₈ homologue. The C₄, C₆, and C₈ FASA were identified at CL 1a with reference standards. The C₃ and C₅ FASA were identified at CL 2c with the aid of homologue evidence and partly due to the low amount of diagnostic fragments inherent to FASA. FASA have been detected previously in matrices such as wastewater originating from 3M factories [40]. It is also known to occur at AFFF impacted sites where it believed to be an intermediate transformation product originating from a more complex structure but has been left with a sulfonamide head group [41,42].

Another AFFF derived PFAS is the group of N-methyl perfluoroalkane sulfonamidoacetic acids (Me-FASAA, ID 17 f), where only the C₈ N-methyl Me-FOSAA was previously included. It was identified here at CL 1a using a reference standard (Fig. S2 in SI). The C₃, C₄, C₅, and C₆ Me-FOSAA homologues were identified at CL 2b, due to the amount of diagnostic ions found in the MS² data (Fig. S2 in SI). The group N-ethyl (Et-FASAA, ID 18 f) had a similar spread of carbon chain lengths (C₄, C₅, C₆, C₈ Et-FASAA). Once again, only the C₈ form was previously included and was identified here at CL 1a using a reference standard. The homologues were confirmed at the same CL as the Me-FASAA (CL 2b), due to the strong diagnostic evidence found in the MS² data (Fig. S3 in SI). Me- and Et-FASAA have been detected previously in matrices such as urban runoff water, groundwater, and soil ([43]; T. V. [44]).

Of the remaining six PFAS classes identified with suspect screening, none was included in the targeted method used in the previous study [13].

First, two hydro-substituted perfluoroalkane sulfonic acids (H-PFSA, ID 9 f) were detected in the samples (Fig. S4 in SI). C₄ H-PFSA was confirmed at CL 2a by comparing the mass spectra against data found in the literature (T. [45]), whereas C₆ H-PFSA was confirmed at CL 3a. The most notable fragment was the C₃F₅ ion and the fragmentation did not follow the repeated loss of CF₂/CFH pattern but instead created a perfluoroalkene fragment, as reported previously [45]. There was also no observable HF loss in the spectra, contradicting previous findings [46], most likely due to the low abundance of ions acquired from samples. H-PFSA has been reported previously in groundwater, surface water, and sediment (T. [45,46]).

Second, three perfluoroalkyl ether sulfonic acids (PFESA, ID 10 f) were detected in the samples (Fig. S5 in SI). Two of these contained three perfluorocarbons, but with the ether group located at different positions. The two isomers were not baseline-separated, but the chromatograph clearly showed that these were two separate isomers and this was confirmed using MS² data. The first eluting peak had the ether group separated to the terminal CF₃ and the rest of the perfluorocarbon chain, which was highlighted by the lone fragment matching in accurate mass of CF₃O⁺. The second eluting peak gave a match with the accurate mass of the fragment matching C₂F₅O⁺. The third PFESA contained five fluorine saturated carbons, with the ether located before the terminal CF₃ group. Both PFESA with an ether group located next to the terminal CF₃ showed the same fragment (CF₃O⁺). PFESA have been detected previously [47,48].

Third, three AFFF-derived PFAA precursors, N-SPAmP-FHxSA, N-SPAmP-FHxSAA, and N-SPAmP-FHxSAPS (ID 19 f, 20 f, and 21 f), were detected (Fig. S6, S7 and S8 in SI). All spectra were compared with literature values to confirm the structure [49], which made it possible to identify them at CL 2a.

Fourth, keto-PFSA (ID 14 f) were detected with a perfluorocarbon chain of C₆, C₇, and C₈, at CL 3a for all three homologues (Fig. S9 in SI). Perfluoroalkene anions (C₅F₉⁻ and C₃F₅⁻) were observed in the mass spectrum, indicating a double bond formed at the terminal carbon. One

Table 1Summary of results of suspect and non-target screening of PFAS: ID, class name, structure, number of CF₂ moieties (where applicable), and confidence level (CL).

ID	Class name	Structure	n	CL
1 f	PFCA		3 – 9	1a; 1a; 1a; 1a; 1a; 1a; 1a
2 f	PFSA		2 – 7	2a; 1a; 1a; 1a; 1a; 1a
3 f	n:2 FTSA		3; 5; 7	1a; 1a; 1a
4 f	PFECHS		-	1a; 3a; 3a
5 f	PFMCHS		-	3a
6 f	PFCHS		-	2b
7 f	FASA		2 – 5; 7	3c; 1a; 3c; 1a; 1a
8 f	FASHN		3 - 5	2b; 2b; 2b
9 f	H-PFSA		2; 4	2a; 3a; 3a
10 f	PFESA		2 - 4	2a; 2a; 2a
11 f	MeOH-FHxSA		-	2b

(continued on next page)

Table 1 (continued)

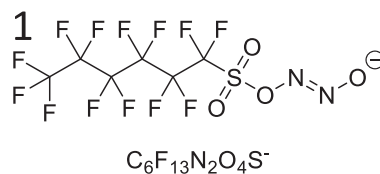
ID	Class name	Structure	n	CL
12 f	PFOCHS		-	3a
13 f	Me-FASASiA		3 – 5	3b; 3b; 3b
14 f	Keto-PFSA		5 - 7	3a; 3a; 3a
15 f	DUPFOS		3	3b
16 f	FASASA		5; 7	2c; 2c
17 f	Me-FASAA		2 – 5; 7	2b; 2b; 2b; 2b; 1a
18 f	Et-FASAA		3–5; 7	2b; 2b; 2b; 1a
19 f	N-SPAmP-FHxSA		-	2a
20 f	N-SPAmP-FHxSAA		-	2a

(continued on next page)

Table 1 (continued)

ID	Class name	Structure	n	CL
21 f	N-SPAmP-FHxSAPS		-	2a
22 f	Bistriflimide		-	2b

FASHN
FH_xHSN



No.	Found m/z	Expected m/z	Error (ppm)	Error (mDa)
1	442.93768	442.93767	0.02	0.01
2	398.93661	398.9366	0.03	0.01
3	98.95615	98.95577	3.84	0.38
4	82.96086	82.96085	0.12	0.01
5	79.95742	79.95736	0.75	0.06
6	77.96558	77.96552	0.77	0.06

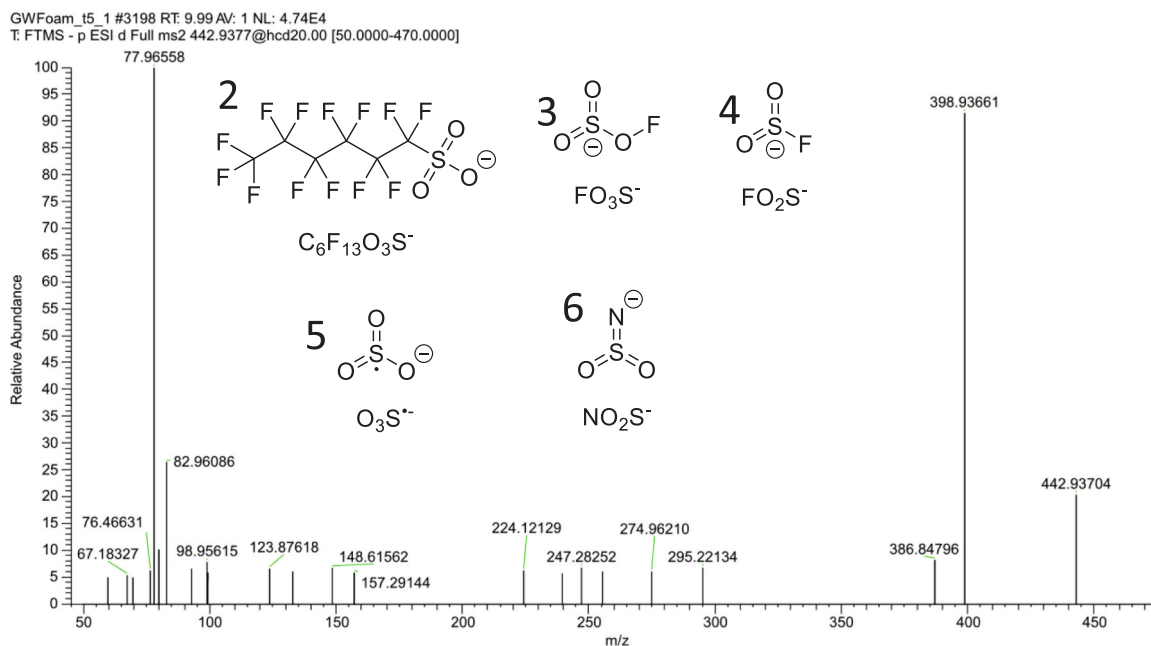


Fig. 2. Annotated mass spectrum of perfluorohexane sulfonylhydrazide (FHxHSN) showing the potential structure of the parent ion and the resulting fragments.

peak in particular implied that the functional group in question was an aldehyde with a neutral loss corresponding to loss of CF_2O . However, this peak was close to the noise level and only appeared in one of the homologues. Low-intensity and irregular mass spectra have been reported previously for this compound group [50,51].

The remaining two classes each only included one single compound. Perfluorooctane dienoic sulfonic acid (DUPFOS, ID 15 f) was detected (Fig. S10 in SI), but due to lack of diagnostic ions the exact positions of the double bonds could not be determined. A fragment consisting of C_8F_{13} , giving more information than MS1 alone, indicated that the compound was at the very least unsaturated in two places. Due to this lack of information, the CL was 3b. Only one previous study has detected this compound, in an AFFF formulation [52].

Another compound, known commercially as Bistriflimide (ID 22 f), was identified (Fig. S11 in SI). The compound is characterized by a central amide with SO_2 groups on each side, which is bonded to terminal CF_3 . Although the molecule is small, the fragments obtained through MS2 data can be considered diagnostic, and as such it was identified at CL 2b. Bistriflimide is used as a reagent and catalyst in organic synthesis [53].

3.2. Structural and prioritization results from non-target screening

Non-target screening yielded two new classes of PFAS and four individual PFAS which, to the best of our knowledge, have never been reported previously, are not included in any suspect list, and have not been proposed in any previous study. These completely new and unreported compounds were in fact transformation products which developed during EO, indicating that entirely new structures can be created in remediation technologies.

In total, the non-target screening process yielded nine individual PFAS which were not present in any of the suspect lists used in the study. These included FASHN (ID 8 f), MeOH-FASA (ID 11 f), Me-FASASiA (ID 13 f), and FASASA (ID 16 f), where the classes FASHN and MeOH-FASA have not been reported previously. The other classes discovered in non-target screening prioritization have been reported previously [41,54], but new homologues were discovered in these classes, extending previous findings.

The first class of new compounds discovered (CL 2b) comprised perfluoroalkyl sulfonate hyponitrites (FASHN, ID 8 f) with perfluoro-carbon chain length ranging from C_4 to C_6 . The annotated spectrum of the C_6 homologue, perfluorohexane sulfonhyponitrite (FHxSHN), is shown in Fig. 2. Some fragments in the fragment library were the parent ions of the various chain lengths of PFSA, which were formed on neutral loss of N_2O^- as a transformation product created in the EO process (see Section 3.4.1).

The second new class of compounds, which also was determined to be formed during EO, was N-methanol perfluoroalkyl sulfonamide (MeOH-FASA) with C_6 chain length (MeOH-FHxSA; Fig. S12 in SI). The two pieces of evidence which led to derivation of this structure were the mass of the neutral loss and the fragment at ~ 107 m/z , indicating CHNO_3S as the functional head group. The most likely configuration in this case is a sulfonamide with an unsaturated carbon bonded to an alcohol, hence the name MeOH-FASA. No homologues were detected and only C_6 MeOH-FASA was identified at CL 2b.

Other compound groups detected are better classified as emerging classes of environmental pollutants rather than completely new PFAS, as they have been reported previously [41,54,55]. However, the complementary information provided here demonstrates that additional isomers and homologues should be included in future studies. Therefore, information about the characteristic fragments is provided here to confirm and expand current knowledge.

The first class of emerging PFAS discovered was named perfluoroalkyl sulfonamide sulfonic acid (FASASA, 16 f) with two homologues in this class, namely C_6 and C_8 , at CL 2c (Fig. S13 in SI). The most stable and intense peak in the mass spectrum was a m/z corresponding to

FHxSA, which resulted from a neutral loss determined to be SO_3 . This resulted in an observed m/z of a FHxSA and FOSA for C_6 and C_8 , respectively. Additional evidence that the feature contained nitrogen was the peak at 77.96552 m/z , which corresponds to a molecular formula of SO_2N^- and is commonly found in FASA and other PFAS containing sulfonamide functional groups. The data obtained with collision energies at 10 and 30 eV did not yield any peaks with only the perfluoroalkyl backbone. However, when the collision energy was increased to 50 eV, C_2F_5 and C_3F_7 peaks were observed, further confirming the annotation. Although the head group of this class seems unorthodox, it has previously been synthesized in production of Zinc-Enzyme inhibitors [56]. It was detected in a recent study analyzing AFFF-impacted groundwater [54], which was the first to report the C_6 homologue, a finding now complemented by our discovery of the C_8 homologue.

Another class of emerging compounds with m/z of 475.93005 was discovered (Fig. S14 in SI). On elucidating the structure of this compound, it was determined to be an n-methyl perfluoroalkyl sulfonamide sulfinic acid (Me-FASASi) previously described in the literature as "methyl((perfluorohexyl)sulfonyl)sulfuramidous acid" [41]. However, Dewapriya et al. [41] discovered only two homologues, namely C_6 and C_8 , whereas we identified C_4 , C_5 , and C_6 homologues. Additionally, this class of PFAS has only previously been detected in blood serum samples obtained from cattle [41], and our study is the first to detect it in aqueous samples.

The third class of emerging compounds discovered had a theoretical m/z of 440.94717 (Fig. S15 in SI). It has been reported in a previous publication as a type of fluorotelomer [55]. However, our results indicated that this feature is in fact a cyclic isomer (see compound ID 11 f in Table 1). The main evidence indicating a cyclic structure was the low amount of CF_2 losses and the fact that the longest perfluoroalkyl chain detected was a C_3F_5 peak. Additionally, most of the peaks detected by Hensema et al. (2020) were not detected in any MS² data in our study. However, the ring opening is not well described by the detected fragments (Fig. S15 in SI) and the compound of concern has not been confirmed with authentic reference standards.

3.3. Suspect screening of chlorinated and brominated compounds

A total of 12 chlorinated and two brominated compounds were detected and confirmed at CL 3 or above using the conventional Schymanski scale for assigning CL [35]. All compounds with CL 2a were confirmed using the Massbank mass spectrum record, which includes aromatic chlorinated transformation products, brominated transformation products, ordinary chlorinated micropollutants, and ordinary brominated micropollutants. No compounds which contained both chlorine and bromine in the same structure were detected. One compound detected (1,2,2-trichloroethanesulfonic acid) was not present in any of the suspect lists, so it had to be manually annotated. Mass spectrometry evidence and a discussion of compounds not identified as EO transformation products are provided in SI.

1,2,2-Trichloroethane sulfonic acid (ID 1c) is a highly chlorinated compound which was not present in any suspect list, but the fragments gave enough information to confirm it at CL 2b (Fig. S16 in SI). This compound has not been reported previously, to the best of our knowledge. The structure was determined based on the fragment observed at 114.92658 m/z , which with the aid of an elemental composition calculator was calculated to be an SO_3Cl^- ion. Based on this, the elemental composition of the compound was calculated to be $\text{C}_2\text{Cl}_3\text{SO}_3\text{H}$.

3,5-Dichlorosalicylic (ID 3c) acid was detected using the suspect list from Massbank (Fig. S17 in SI). There were many different isomers, but only one matched the spectral library obtained from Massbank at CL 2a. 3,5-Dichlorosalicylic acid is a bioactive compound used as a primer to start a defensive reaction in plants [57]. It has also been detected previously as a byproduct after EO treatment [58], as further discussed in

Section 3.4.2 below.

Three nitro-substituted phenyl compounds were detected, all of which were determined to be transformation products. This class of compounds was not well defined due to the absence of any Massbank records for the proposed structures. 2,6-Dichloro-4-nitrophenol (ID 4c) was detected through the suspect list (Fig. S18 in SI). This compound was not available in any spectral library that we accessed and could only be confirmed at CL 3. 2,6-Dichloro-4-nitrophenol is an intermediate in chemical synthesis and a disinfection byproduct [59]. It has been reported previously in various matrices such as seawater and drinking water ([60]; J. [61]). 2-Chloro-4,6-dinitrophenol (ID 7c) was determined at CL 3 (Fig. S19 in SI). It is a supplement used in culture medium for growth of microorganisms and has been reported previously in wastewater [62,63]. 4-Chloro-3-nitrobenzenesulfonic acid (10c) was identified at CL 3 (Fig. S20 in SI). It is a reagent used for preparation of 2-chloro-3-bromoaniline [64]. It is included in a suspect list made through *in-silico* predictions of phase 1 human metabolites [65].

3-[(2-Chlorophenyl)amino]-3-oxopropanoic acid (ID 6c), which was detected with the suspect list, did not have any spectral record in Massbank with CL 3 (Fig. S21 in SI). This compound has a data quality level of 5 on the CompTox Chemicals Dashboard, which is “programmatically curated from ACToR or PubChem, unique chemical identifiers with low confidence, single public source” with no reliable source available [66].

Only two brominated compounds were identified in suspect screening and both were determined to be transformation products. One of these, 2,4-dinitro-6-bromophenol (ID 1b), had very few fragments that could be considered diagnostic and the exact positions of the functional groups on the benzene could not be determined, so it was given CL 3 (Fig. S22 in SI). It is a precursor to brominated aniline derivatives and is hypothesized to be a potential breakdown product of tetrabromobisphenol A [67,68]. The other brominated compound detected in suspect screening was 3,5-dibromo-4-hydroxybenzoic acid (ID 2b), at CL 3 (Fig. S23 in SI). It is a secondary plant metabolite and has been reported previously in rivers downstream of industrial waste water effluents ([69]; H. H. [70]).

3.4. Transformation products

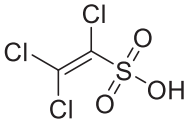
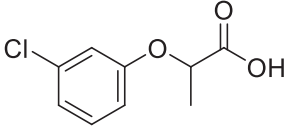
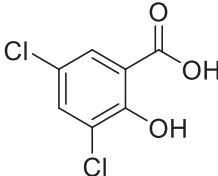
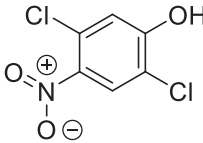
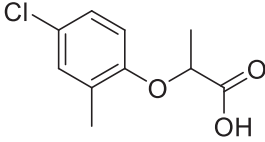
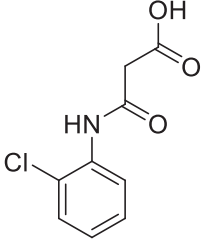
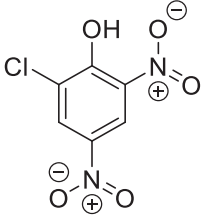
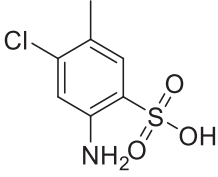
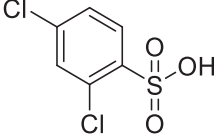
3.4.1. PFAS transformation products

Three different groups of PFAS were detected during EO and classified as (i) detected at all or almost all time points during EO at the same intensity, (ii) decreasing normalized area during EO, indicating mineralization or transformation of the compound into transformation products, or (iii) PFAS transformation products not detected at $t = 0$ and formed during EO (Fig. 3). The PFAS classes detected at all time points were PFESA (only the shortest homologue, ID 10 f, with some exceptions), Keto-PFSA (ID 14 f), and DUPFOS (ID 15 f), indicating that these persistent PFAS were resistant to the EO process applied in this study. The PFAS classes which showed decreasing levels were PFOCHS (ID 12 f), Me-FASASi (ID 13 f), FASASA (ID 16 f), Me-FASAA (ID 17 f), Et-FASAA (ID 18 f), N-SPAmP-FHxSA (ID 19 f), N-SPAmP-FHxSAA (ID 20 f), N-SPAmP-FHxSAPS (ID 21 f), and Bistriflimide (ID 22 f). The decreasing concentrations indicate that these compounds were either changed into transformation products or mineralized, as shown previously for PFCA and PFSA [71,72]. The third class of PFAS created during the EO process included FASHN (ID 8 f), H-PFSA (ID 9 f), and PFPrES in the PFESA (ID 10 f).

An increase in nitrate, originating from oxidation of ammonia during EO, may explain the formation of FASHN (Fig. 4). The hyponitrous acid group (N_2O_2H -group) of FASHN could be explained by the high concentration of nitrate, which in groundwater samples increased from below 1 mg L^{-1} to $6\text{--}8 \text{ mg L}^{-1}$ after EO treatment in our previous study [13]. The high oxidation potential of the boron-doped diamond may have resulted in formation of hyponitrous acid, as an intermediate in ammonia oxidation that can be nucleophilically substituted on the

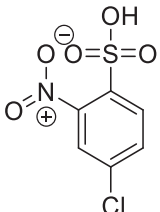
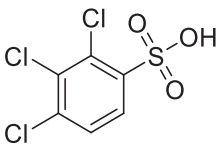
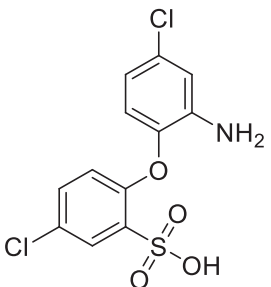
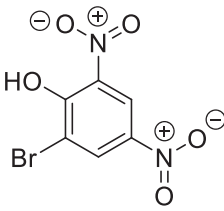
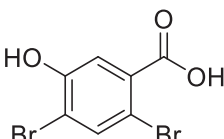
Table 2

Summary of results of suspect screening of chlorinated and brominated compounds: ID, class name, structure, and confidence level (CL).

ID	Name	Structure	CL
1c	1,2,2-Trichloroethane-sulfonic acid		2b
2c	Chlorprop		2a
3c	3,5-Dichlorosalicylic acid		3
4c	2,6-Dichloro-4-nitrophenol		3
5c	Mecoprop		2a
6c	3-[(2-Chlorophenyl)amino]-3-oxopropanoic acid		3
7c	2-Chloro-4,6-dinitrophenol		3
8c	2-Chloro-4-aminotoluene-5-sulfonic acid		3
9c	2,5-Dichlorobenzene-sulfonic acid		3

(continued on next page)

Table 2 (continued)

10c	4-Chloro-3-nitrobenzenesulfonic acid		3
11c	2,3,4-Trichlorobenzenesulfonic acid		2b
12c	2-(2-Amino-4-chlorophenoxy)-5-chlorobenzene-sulfonic acid		3
1b	2,4-dinitro-6-bromophenol		3
2b	3,5-Dibromo-4-hydroxybenzoic acid		3

sulfonic acid head-group. We base this hypothesis on fundamental data on ammonia oxidation showing that one of the intermediate oxidation products is hyponitrous acid [73].

Although FASASA was not identified as a transformation product in EO treatment, we highlight it as a compound of emerging concern. A previous study showed that compounds with the FASASA head group ($C_6F_5SO_2NHSO_3H$ & $3-CF_3-C_6H_4SO_2NHSO_3H$) can be synthesized from alkylsulfonyl halides and sulfamic acid, in the presence of 1 N NaOH [74]. We hypothesize that the presence of sulfamic acid, which has been detected in wastewater treatment plant effluent around Europe at concentrations up to 1.6 ppm [75], led to the formation of FASASA-type compounds in the landfill from which our leachate samples originated. Sulfamic acid has also been detected in Canadian municipal landfill sites and we believe that it is likely then to also be present in this landfill [76].

MeOH-FHxSA (ID 11 f) was detected after one hour of EO treatment, but not after 3 h or at any other time point. The most likely reason, based on the structure determined for this compound, was incomplete degradation of e.g., N-SPAmP-FHxSAA, Et-FASAA, or Me-FASAA. Common transformation products that occur normally during natural degradation are N-ethyl (Et-FOSE) and N-methyl perfluoroalkyl sulfonamido ethanols (Me-FOSE), which are very close in structure to MeOH-FHxSA (J. [77]). A carboxylic acid functional group is located on the amide for N-SPAmP-FHxSAA, as also observed for Et-FHxSAA and Me-FHxSAA.

These could be converted to alcohols through a hydroxyl substitution on the carbon bonded to the amide combined with alkyl cleavages (Fig. 4).

H-PFSA were also determined to be a transformation product, as they were only detected in treated samples. However, the branched isomer of H-PFHxS was detected at $t = 0$ in every sample matrix. This class of PFAS is known to occur in biota and other environmental matrices such as groundwater, wastewater, and AFFF impacted soils. ([41,55]; T. [78, 79]). Detection of H-PFSA in our samples may indicate a new pathway for formation of hydrogen-substituted PFAS in aqueous samples. Only H-PFSA were detected here, but other terminal PFAS products such as H-PFCA should not be ignored and may be detected in other EO studies.

PFESA were not detected at $t = 0$ of EO treatment in one of the four matrices analyzed (leachate water), while in the other three matrices PFPeES and PFBES were detected at $t = 0$. On the other hand, PFPRES was never detected at $t = 0$, but at the earliest after 3 h of EO treatment. It is possible that chain shortening of longer-chain PFESA occurred, since the intensity of shorter-chain PFESA increased from 0 to 3 h of EO treatment. This is consistent with the mechanism of EO treatment, which results in chain shortening [16].

Me-FASASiA was detected in groundwater sample at $t = 0$, whereas it was not detected in leachate water at $t = 0$, but appeared after 1 h of EO treatment. It is possible that this class was simply not detected at $t = 0$ in the leachate samples due to low concentrations or matrix effects, rather than being formed during EO. This class of PFAS has been detected in biota [41], but was detected in aqueous samples for the first time in this study.

3.4.2. Chlorinated and brominated transformation products

There was a clear trend for all transformation products, except 3,5-dibromo-4-hydroxybenzoic acid and 3-[(2-chlorophenyl)amino]-3-oxopropanoic acid, to contain nitro groups, due to the increase of nitrate after EO (see Section 3.4.1). Introduction of nitrate radicals into a system has previously been shown to produce nitrate-containing organics, with nitro-substitution as a transformation pathway [80]. Another interesting finding was that these transformation products were often created, but then began breaking down. This indicates that nitrate was not the limiting reagent for their formation, since it was still present after the treatment.

In the EO-treated groundwater foam, nitro-phenols (2,6-dichloro-4-nitrophenol, 2-chloro-4,6-dinitrophenol, and 2,4-dinitro-6-bromophenol; ID 4c, 7c, and 1b) were not detected until after $t = 5$ h, whereas these compounds were detected at $t = 3$ h in the EO-treated groundwater (Fig. 5). The time of highest intensity for these transformation products also differed between the EO-treated groundwater and groundwater foam (Fig. 5). Two out of three transformation products were present in their highest concentration in the EO-treated groundwater at $t = 5$ h, but in the EO-treated groundwater foam at $t = 7$. Thus either the foam fractionation pre-treatment did not efficiently concentrate the precursors needed for formation of these transformation products, or the foam matrix limited the rate of reaction. This slower formation means that the foam fractionation step could create a rate-limiting matrix, where pre-concentration of PFAS causes some chlorinated and brominated compounds to be less efficiently oxidized. 3,5-dichlorosalicylic acid has been reported previously as a byproduct of EO [58], but in our study it was detected before treatment and the concentration increased as more was formed during EO treatment.

This study demonstrated formation of transformation products during EO treatment, which occurred as a direct result of the treatment. The toxicity of the newly formed compounds need to be investigated in the future. However, in our previous study [13] we included effect-based analyses, namely transthyretin (TTR)-binding assays and *A. fischeri* bioluminescence assays. The TTR binding assay uses endocrine disruption as its endpoint, while the bioluminescence assay is a measure of general toxic potency. The activity (toxicity) of the water decreased strongly (~ 90 %) after electrochemical treatment for both assays [13],

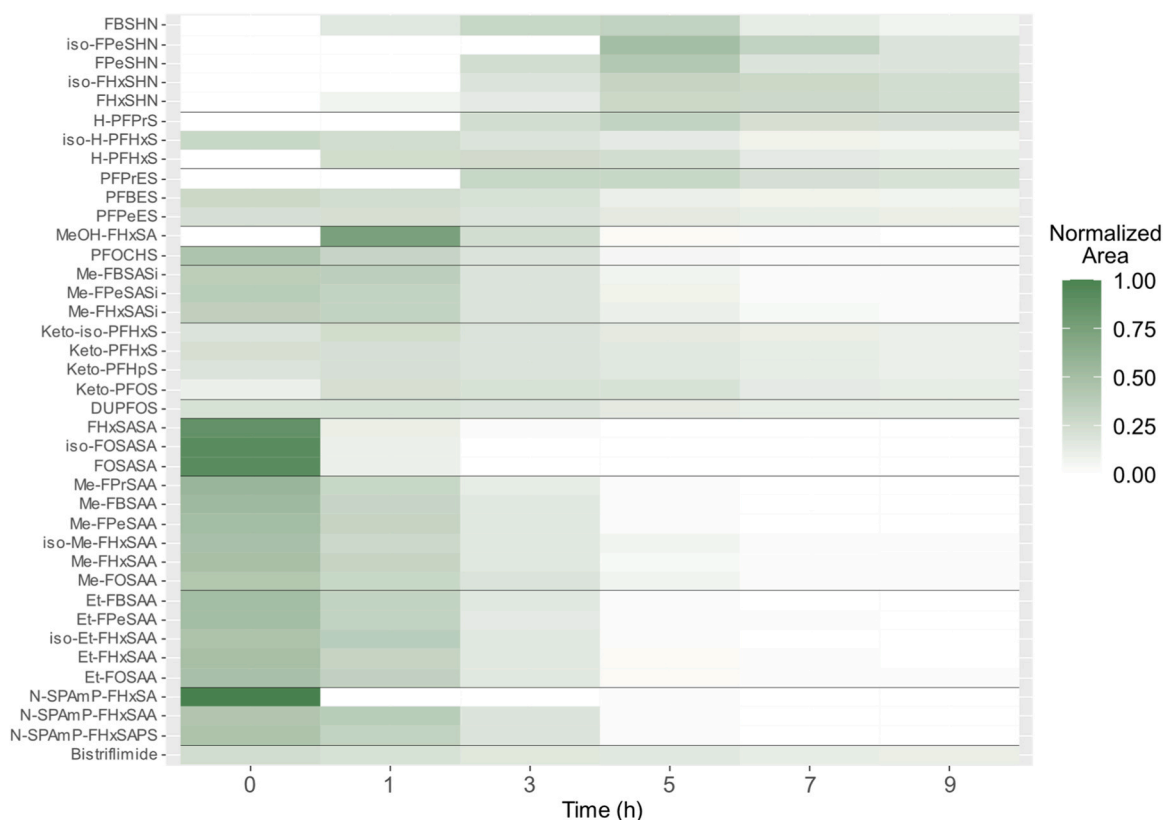


Fig. 3. Heat map of per- and polyfluoroalkyl substances (PFAS) detected in suspect and non-target screening of enriched foam obtained from groundwater after 0, 1, 3, 5, 7, and 9 h of electrochemical oxidation (EO) treatment. A compound with an “iso-” prefix is a branched isomer which eluted before the linear isomer.

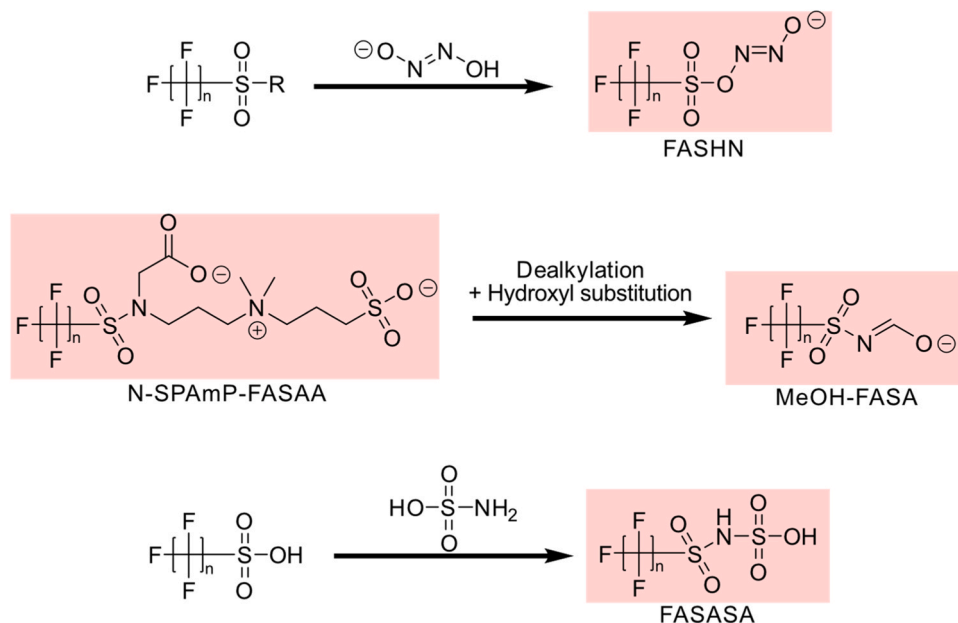


Fig. 4. Proposed formation pathway of (top to bottom) FASHN, FASASA, and MeOH-FASA, three new classes of per- and polyfluoroalkyl substances (PFAS) discovered in this study. Compound structures marked in pink boxes were detected and structure was determined at confidence level (CL) 3d or above.

indicating that the activity of the transformation products was negligible compared with that of the original pollutants. However, the toxicity of the untreated water could not be explained solely by the originally measured target PFAS, and hence the compounds identified here may have partly caused the bioassay activity at time zero.

In addition to contamination of the aqueous environment, there may

be a risk of emitting unknown transformation products (products of incomplete destruction, reactions occurring with the matrix, etc.) to the air. Little is known about this, necessitating further research on the water treatment techniques currently used. What is known is currently is the risk of producing short chain PFAS which although not as bio-accumulative, might still be toxic due to their ubiquity in the

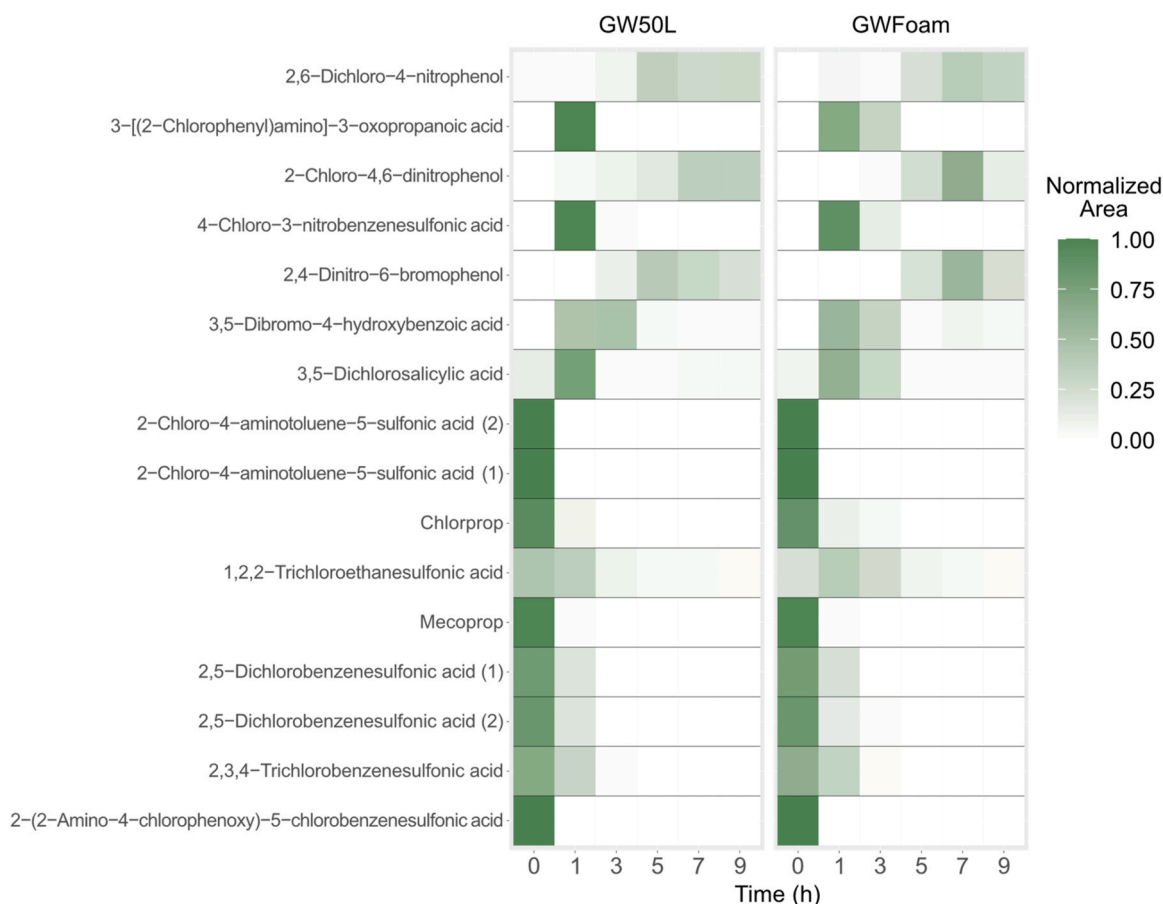


Fig. 5. Heat map of chlorinated and brominated compounds identified during suspect screening after 0, 1, 3, 5, 7, and 9 h of electrochemical oxidation (EO) treatment in (left) 50 L of groundwater (GW50L) treated with EO and (right) groundwater foam (GWFoam) pre-treated with foam fractionation and then treated with EO.

environment. Furthermore, techniques such as GAC and foam fractionation are less effective at removing short chain PFAS [16,26]. The risk of emitting airborne contaminants should also be investigated. Effect-directed analyses could be used for identification of such toxic compounds [81], by combining appropriate bioassays with non-targeted screening techniques.

4. Conclusions

PFAS, chlorinated and brominated compounds, and their transformation products were identified in landfill leachate and groundwater treated with EO, with or without foam fractionation as a pre-concentration step. Thus while EO treatment may have the potential to destroy PFAS, there is an associated risk of formation of transformation products. More studies are needed to determine their concentrations and their toxicity. This study revealed that ammonia is oxidized during EO, so formation of nitrate and nitrate radicals might be one of the contributing factors to formation of N-containing transformation products. Literature has found that halogenated nitrogenous disinfection byproducts are more toxic disinfection byproducts that are only halogenated [82].

Suspect and non-target screening proved to be appropriate techniques for exploring the chemical space created by destructive treatment of PFAS. Two new classes of PFAS (FASHN and MeOH-FASA) were discovered for the first time, one of which included transformation products (FASHN). These transformation products were possibly formed through a substitution reaction of hyponitrous acid, with this functional group becoming the new head group of a PFAS. Detection of H-PFSA revealed a potential new pathway for its formation during EO treatment.

Six chlorinated or brominated compounds formed during EO treatment were detected, and pre-treatment with foam fractionation seemed to affect formation and/or degradation of these compounds.

These findings highlight the need to monitor transformation products during EO treatment and the importance of suspect and non-targeted screening tools. Further studies are needed to identify transformation products arising in novel destructive treatment technologies being developed in response to stricter PFAS regulations in drinking water and other aqueous matrices. Previous bioassays indicate that the transformation products identified here are unlikely to be significantly biologically active, but it is possible that previously unidentified PFAS present before treatment modified the biological effect in the matrices tested.

Environmental implication

This study focuses on the identification of PFAS and other halogenated compounds, and their transformation products using electrochemical oxidation (EO) on landfill leachate and groundwater. The development of advanced treatment methods can reduce the potential threat of these compounds to environmental and human health. In this study potentially toxic transformation products are formed during the EO treatment process, which can be potential environmental hazards. Additionally, we could show that the water matrix plays an important role in the types of chemicals that can be formed. This study contributes to a better evaluation of advanced treatment method for removal of hazardous pollutants.

CRedit authorship contribution statement

Sanne J Smith: Writing – review & editing, Validation, Supervision, Resources, Investigation. **Lutz Ahrens:** Writing – review & editing, Supervision, Resources, Funding acquisition. **Svante Rehnstam:** Writing – original draft, Visualization, Software, Investigation, Formal analysis.

Declaration of Competing Interest

The authors declare that they have no known competing financial interests or personal relationships that could have appeared to influence the work reported in this paper.

Appendix A. Supporting information

Supplementary data associated with this article can be found in the online version at [doi:10.1016/j.jhazmat.2024.136316](https://doi.org/10.1016/j.jhazmat.2024.136316).

Data Availability

Data will be made available on request.

References

- Baderna, D., Maggioni, S., Boriani, E., Gemma, S., Molteni, M., Lombardo, A., et al., 2011. A combined approach to investigate the toxicity of an industrial landfill's leachate: chemical analyses, risk assessment and in vitro assays. *Environ Res* 111 (4), 603–613. <https://doi.org/10.1016/j.envres.2011.01.015>.
- Bakare, A.A., Mosuro, A.A., Osibanjo, O., 2000. Effect of simulated leachate on chromosomes and mitosis in roots of *Allium cepa* (L.). *J Environ Biol* 21 (3), 263–271 <https://www.scopus.com/inward/record.uri?eid=2-s2.0-0033896486&partnerID=40&md5=323f013ee02e0daf12e351ebde0510a>.
- El-Fadel, M., Findikakis, A.N., Leckie, J.O., 1997. Environmental impacts of solid waste landfilling. *J Environ Manag* 50 (1), 1–25. <https://doi.org/10.1006/jema.1995.0131>.
- Renou, S., Givaudan, J.G., Poulain, S., Dirassouyan, F., Moulin, P., 2008. Landfill leachate treatment: review and opportunity. *J Hazard Mater* 150 (3), 468–493. <https://doi.org/10.1016/j.jhazmat.2007.09.077>.
- Mohammad-pajooh, E., Turcios, A.E., Cuff, G., Weichgrebe, D., Rosenwinkel, K.H., Vedenyapina, M.D., et al., 2018. Removal of inert COD and trace metals from stabilized landfill leachate by granular activated carbon (GAC) adsorption. *J Environ Manag* 228 (September), 189–196. <https://doi.org/10.1016/j.jenvman.2018.09.020>.
- Hamid, H., Li, L.Y., Grace, J.R., 2018. Review of the fate and transformation of per- and polyfluoroalkyl substances (PFASs) in landfills. *Environ Pollut* 235, 74–84. <https://doi.org/10.1016/j.envpol.2017.12.030>.
- Bell, E.M., De Guise, S., McCutcheon, J.R., Lei, Y., Levin, M., Li, B., et al., 2021. Exposure, health effects, sensing, and remediation of the emerging PFAS contaminants – Scientific challenges and potential research directions. *Sci Total Environ* 780, 146399. <https://doi.org/10.1016/j.scitotenv.2021.146399>.
- Glüge, J., Scheringer, M., Cousins, I.T., Dewitt, J.C., Goldenman, G., Herzke, D., et al., 2020. An overview of the uses of per- And polyfluoroalkyl substances (PFAS). *Environ Sci: Process Impacts* 22 (12), 2345–2373. <https://doi.org/10.1039/d0em00291g>.
- Gagliano, E., Sgroi, M., Falciglia, P.P., Vagliasindi, F.G.A., Roccaro, P., 2020. Removal of poly- and perfluoroalkyl substances (PFAS) from water by adsorption: Role of PFAS chain length, effect of organic matter and challenges in adsorbent regeneration. *Water Res* 171, 115381. <https://doi.org/10.1016/j.watres.2019.115381>.
- Veciana, M., Bräunig, J., Farhat, A., Pype, M.L., Freguia, S., Carvalho, G., et al., 2022. Electrochemical oxidation processes for PFAS removal from contaminated water and wastewater: fundamentals, gaps and opportunities towards practical implementation. *J Hazard Mater* 434 (December 2021). <https://doi.org/10.1016/j.jhazmat.2022.128886>.
- Xu, B., Liu, S., Zhou, J.L., Zheng, C., Weifeng, J., Chen, B., et al., 2021. PFAS and their substitutes in groundwater: Occurrence, transformation and remediation. *J Hazard Mater* 412, 125159. <https://doi.org/10.1016/j.jhazmat.2021.125159>.
- Kucharzyk, K.H., Darlington, R., Benotti, M., Deeb, R., Hawley, E., 2017. Novel treatment technologies for PFAS compounds: a critical review. *J Environ Manag* 204, 757–764. <https://doi.org/10.1016/j.jenvman.2017.08.016>.
- Smith, S.J., Lauria, M., Ahrens, L., McCleaf, P., Hollman, P., Bjälkefur Seroka, S., et al., 2023. Electrochemical oxidation for treatment of PFAS in contaminated water and fractionated foam—a pilot-scale study. *ACS EST Water*. <https://doi.org/10.1021/acsestwater.2c00660>.
- Wang, Y., Ji, Y., Li, K., Huang, Q., 2023. Foam fractionation and electrochemical oxidation for the treatment of per- and polyfluoroalkyl substances (PFAS) in environmental water samples. *Chemosphere* 339 (May). <https://doi.org/10.1016/j.chemosphere.2023.139615>.
- We, A.C.E., Zamyadi, A., Stickland, A.D., Clarke, B.O., Freguia, S., 2024. A review of foam fractionation for the removal of per- and polyfluoroalkyl substances (PFAS) from aqueous matrices. *J Hazard Mater* 465 (ember 2023), 133182. <https://doi.org/10.1016/j.jhazmat.2023.133182>.
- Radjenovic, J., Duinslaeger, N., Avval, S.S., Chaplin, B.P., 2020. Facing the challenge of poly- and perfluoroalkyl substances in water: is electrochemical oxidation the answer? *Environ Sci Technol* 54 (23), 14815–14829. <https://doi.org/10.1021/acs.est.0c06212>.
- Horst, J., McDonough, J., Ross, L., Houtz, E., 2020. Understanding and managing the potential by-products of PFAS destruction. *Groundw Monit Remediat* 40 (2), 17–27. <https://doi.org/10.1111/gwrm.12372>.
- Smith, S.J., Lauria, M., Higgins, C.P., Pennell, K.D., Blotvogel, J., Arp, H.P.H., 2024. The need to include a fluorine mass balance in the development of effective technologies for PFAS destruction. *Environ Sci Technol* 1c. <https://doi.org/10.1021/acs.est.3c10617>.
- Gar Alalm, M., Boffito, D.C., 2022. Mechanisms and pathways of PFAS degradation by advanced oxidation and reduction processes: A critical review. *Chem Eng J* 450 (P4), 138352. <https://doi.org/10.1016/j.cej.2022.138352>.
- Hollender, J., Schymanski, E.L., Ahrens, L., Alygizakis, N., Béen, F., Bijlsma, L., et al., 2023. NORMAN guidance on suspect and non-target screening in environmental monitoring. In: *Environmental Sciences Europe*, 35. Springer Berlin Heidelberg. <https://doi.org/10.1186/s12302-023-00779-4>.
- Menger, F., Gago-Ferrero, P., Wiberg, K., Ahrens, L., 2020. Wide-scope screening of polar contaminants of concern in water: A critical review of liquid chromatography-high resolution mass spectrometry-based strategies. *Trends Environ Anal Chem* 28, e00102. <https://doi.org/10.1016/j.teac.2020.e00102>.
- Getzinger, G.J., Higgins, C.P., Ferguson, P.L., 2021. Structure database and in silico spectral library for comprehensive suspect screening of per- and polyfluoroalkyl substances (PFASs) in environmental media by high-resolution mass spectrometry. *Anal Chem* 93 (5), 2820–2827. <https://doi.org/10.1021/acs.analchem.0c04109>.
- Koelmel, J.P., Paige, M.K., Aristizabal-Henao, J.J., Robey, N.M., Nason, S.L., Stelben, P.J., et al., 2020. Toward comprehensive per- And polyfluoroalkyl substances annotation using fluoromatch software and intelligent high-resolution tandem mass spectrometry acquisition. *Anal Chem* 92 (16), 11186–11194. <https://doi.org/10.1021/acs.analchem.0c01591>.
- Koelmel, J.P., Stelben, P., Godri, D., Qi, J., McDonough, C.A., Dukes, D.A., et al., 2022. Interactive software for visualization of nontargeted mass spectrometry data—FluoroMatch visualizer. *Exposome* 2 (1), 35–37. <https://doi.org/10.1093/exposome/osac006>.
- Koelmel, J.P., Stelben, P., McDonough, C.A., Dukes, D.A., Aristizabal-Henao, J.J., Nason, S.L., et al., 2022. FluoroMatch 2.0—making automated and comprehensive non-targeted PFAS annotation a reality. *Anal Bioanal Chem* 414 (3), 1201–1215. <https://doi.org/10.1007/s00216-021-03392-7>.
- Smith, S.J., Wiberg, K., McCleaf, P., Ahrens, L., 2022. Pilot-scale continuous foam fractionation for the removal of per- and polyfluoroalkyl substances (PFAS) from landfill leachate. *ACS Environ Sci Technol Water*. <https://doi.org/10.1021/acsestwater.2c00032>.
- Schulz, W., Landeswasserversorgung, Z., Lucke, T., Oberleitner, D., Balsaa, P., 2019. Use Non-Target Screen LC-ESI-HRMS Water Anal (Guidel-Ed 1, 0 <https://www.researchgate.net/publication/338357752>
- Sanchez, J.M., Tautenhahn, R., 2023. A comprehensive software workflow for nontargeted analysis of per- and polyfluoroalkyl substances (PFAS) by high-resolution mass spectrometry (HRMS). In: *Thermo Fischer Scientific*.
- Kaufmann, A., Butcher, P., Maden, K., Walker, S., Widmer, M., 2022. Simplifying nontargeted analysis of PFAS in complex food matrices. *J AOAC Int* 105 (5), 1280–1287. <https://doi.org/10.1093/jaoacint/qsac071>.
- Thermo Fischer Scientific, 2023. User Guide for LC Studies Software Version 3.3 SP2 (Issue March). <https://assets.thermofisher.com/TFS-Assets/CMD/manuals/XCALI-98478-Compound-Discoverer-User-Guide-LC-Studies-XCALI98478-en.pdf>.
- NORMAN Network, 2021. NORMAN Substance Database - NORMAN SusDat (<https://www.norman-network.com/nds/susdat/>).
- NORMAN Network, 2023. NORMAN Substace Database - NORMAN SusDat (<https://www.norman-network.com/nds/susdat/>).
- Rehnstam, S., 2023. PFAS Homol Ser (<https://github.com/SRehns/PFAS-Homologous-series>).
- Charbonnet, J.A., McDonough, C.A., Xiao, F., Schwichtenberg, T., Cao, D., Kaserzon, S., et al., 2022. Communicating confidence of per- and polyfluoroalkyl substance identification via high-resolution mass spectrometry. *Environ Sci Technol Lett*. <https://doi.org/10.1021/acs.estlett.2c00206>.
- Schymanski, E.L., Jeon, J., Gulde, R., Fenner, K., Ruff, M., Singer, H.P., et al., 2014. Identifying small molecules via high resolution mass spectrometry: Communicating confidence. *Environ Sci Technol* 48 (4), 2097–2098. <https://doi.org/10.1021/es5002105>.
- R Core Team, 2022. R: A Lang Environ Stat Comput (<https://www.r-project.org/>).
- Wickham, H., 2022. String: Simple, Consistent Wrappers Common String Oper (<https://cran.r-project.org/package=string>).
- Wickham, H., Averick, M., Bryan, J., Chang, W., McGowan, L., François, R., et al., 2019. Welcome to the Tidyverse. *J Open Source Softw* 4 (43), 1686. <https://doi.org/10.21105/joss.01686>.
- De Silva, A.O., Spencer, C., Scott, B.F., Backus, S., Muir, D.C.G., 2011. Detection of a cyclic perfluorinated acid, perfluoroethylcyclohexane sulfonate, in the great lakes of North America. *Environ Sci Technol* 45 (19), 8060–8066. <https://doi.org/10.1021/es200135c>.

- [40] Boulanger, B., Vargo, J.D., Schnoor, J.L., Hornbuckle, K.C., 2005. Evaluation of perfluorooctane surfactants in a wastewater treatment system and in a commercial surface protection product. *Environ Sci Technol* 39 (15), 5524–5530. <https://doi.org/10.1021/es050213u>.
- [41] Dewapriya, P., Nilsson, S., Ghorbani Gorji, S., O'Brien, J.W., Bräunig, J., Gómez Ramos, M.J., et al., 2023. Novel Per- and Polyfluoroalkyl Substances Discovered in Cattle Exposed to AFFF-Impacted Groundwater. *Environ Sci Technol* 57 (36), 13635–13645. <https://doi.org/10.1021/acs.est.3c03852>.
- [42] Rhoads, K.R., Janssen, E.M.L., Luthy, R.G., Criddle, C.S., 2008. Aerobic biotransformation and fate of N-ethyl perfluorooctane sulfonamidoethanol (N-EtFOSE) in activated sludge. *Environ Sci Technol* 42 (8), 2873–2878. <https://doi.org/10.1021/es702866c>.
- [43] Houtz, E.F., Higgins, C.P., Field, J.A., Sedlak, D.L., 2013. Persistence of perfluoroalkyl acid precursors in AFFF-impacted groundwater and soil. *Environ Sci Technol* 47 (15), 8187–8195. <https://doi.org/10.1021/es4018877>.
- [44] Nguyen, T.V., Reinhard, M., Chen, H., Gin, K.Y.H., 2016. Fate and transport of perfluoro- and polyfluoroalkyl substances including perfluorooctane sulfonamides in a managed urban water body. *Environ Sci Pollut Res* 23 (11), 10382–10392. <https://doi.org/10.1007/s11356-016-6788-9>.
- [45] Liu, T., Hu, Li-X., Han, Y., Dong, L.-L., Wang, Y.-Q., Zhao, J.-H., et al., 2022. Non-target and target screening of per- and polyfluoroalkyl substances in landfill leachate and impact on groundwater in Guangzhou, China. *SSRN Electron J* 844 (April), 157021. <https://doi.org/10.2139/ssrn.4092427>.
- [46] Newton, S., McMahan, R., Stoeckel, J.A., Chislock, M., Lindstrom, A., Strynar, M., 2017. Novel polyfluorinated compounds identified using high resolution mass spectrometry downstream of manufacturing facilities near decatur, Alabama. *Environ Sci Technol* 51 (3), 1544–1552. <https://doi.org/10.1021/acs.est.6b05330>.
- [47] Fernandez, N.A., Rodriguez-Freire, L., Keswani, M., Sierra-Alvarez, R., 2016. Effect of chemical structure on the sonochemical degradation of perfluoroalkyl and polyfluoroalkyl substances (PFASs). *Environ Sci: Water Res Technol* 2 (6), 975–983. <https://doi.org/10.1039/c6ew00150e>.
- [48] McCord, J., Strynar, M., 2019. Identification of per- and polyfluoroalkyl substances in the cape fear river by high resolution mass spectrometry and nontargeted screening. *Environ Sci Technol* 53 (9), 4717–4727. <https://doi.org/10.1021/acs.est.8b06017>.
- [49] Barzen-Hanson, K.A., Roberts, S.C., Choyke, S., Oetjen, K., McAlees, A., Riddell, N., et al., 2017. Discovery of 40 classes of per- and polyfluoroalkyl substances in historical aqueous film-forming foams (AFFFs) and AFFF-impacted groundwater. *Environ Sci Technol* 51 (4), 2047–2057. <https://doi.org/10.1021/acs.est.6b05843>.
- [50] Baduel, C., Mueller, J.F., Rotander, A., Corfield, J., Gomez-Ramos, M.J., 2017. Discovery of novel per- and polyfluoroalkyl substances (PFASs) at a fire fighting training ground and preliminary investigation of their fate and mobility. *Chemosphere* 185, 1030–1038. <https://doi.org/10.1016/j.chemosphere.2017.06.096>.
- [51] McDonough, C.A., Higgins, C.P., Choyke, S., Barton, K.E., Mass, S., Starling, A.P., et al., 2021. Unsaturated PPOS and other PFASs in human serum and drinking water from an aff-impacted community. *Environ Sci Technol* 55 (12), 8139–8148. <https://doi.org/10.1021/acs.est.1c00522>.
- [52] Luo, Y.S., Aly, N.A., McCord, J., Strynar, M.J., Chiu, W.A., Dodds, J.N., et al., 2020. Rapid characterization of emerging per- and polyfluoroalkyl substances in aqueous film-forming foams using ion mobility spectrometry-mass spectrometry. *Environ Sci Technol* 54 (23), 15024–15034. <https://doi.org/10.1021/acs.est.0c04798>.
- [53] Zhao, W., Sun, J., 2018. Triflimide (HNTF2) in organic synthesis. *Chem Rev* 118 (20), 10349–10392. <https://doi.org/10.1021/acs.chemrev.8b00279>.
- [54] Ghorbani Gorji, S., Gómez Ramos, M.J., Dewapriya, P., Schulze, B., Mackie, R., Nguyen, T.M.H., et al., 2023. New PFASs Identified in AFFF impacted groundwater by passive sampling and nontarget analysis. *Environ Sci Technol*. <https://doi.org/10.1021/acs.est.3c06591>.
- [55] Hensema, T.J., Berendsen, B.J.A., van Leeuwen, S.P.J., 2021. Non-targeted identification of per- and polyfluoroalkyl substances at trace level in surface water using fragment ion flagging. *Chemosphere* 265, 128599. <https://doi.org/10.1016/j.chemosphere.2020.128599>.
- [56] Supuran, C.T., Winum, J.-Y., Wang, B., 2009. *DRug Design Of Zinc-enzyme Inhibitors*, 14. John Wiley & Sons, Incorporated., pp. 58–59.
- [57] Hamany Djande, C.Y., Steenkamp, P.A., Piater, L.A., Tugizimana, F., Dubery, I.A., 2023. Metabolic reprogramming of barley in response to foliar application of dichlorinated functional analogues of salicylic acid as priming agents and inducers of plant defence. *Metabolites* 13 (5). <https://doi.org/10.3390/metabo13050666>.
- [58] Ambauen, N., Muff, J., Mai, N.L., Hallé, C., Trinh, T.T., Meyn, T., 2019. Insights into the kinetics of intermediate formation during electrochemical oxidation of the organic model pollutant salicylic acid in chloride electrolyte. *Water* 11 (7). <https://doi.org/10.3390/w11071322>.
- [59] Arora, P.K., Srivastava, A., Garg, S.K., Singh, V.P., 2018. Recent advances in degradation of chloronitrophenols. *Bioresour Technol* 250, 902–909. <https://doi.org/10.1016/j.biortech.2017.12.007>.
- [60] Jiang, J., Zhang, X., Zhu, X., Li, Y., 2017. Removal of intermediate aromatic halogenated dbps by activated carbon adsorption: a new approach to controlling halogenated dbps in chlorinated drinking water. *Environ Sci Technol* 51 (6), 3435–3444. <https://doi.org/10.1021/acs.est.6b06161>.
- [61] Liu, J., Zhang, X., Li, Y., Li, W., Hang, C., Sharma, V.K., 2019. Phototransformation of halophenolic disinfection byproducts in receiving seawater: Kinetics, products, and toxicity. *Water Res* 150, 68–76. <https://doi.org/10.1016/j.watres.2018.11.059>.
- [62] Hughes, B.M., McKenzie, D.E., Duffin, K.L., 1993. Identification of components in waste streams by electrospray and tandem mass spectrometry. *J Am Soc Mass Spectrom* 4 (7), 604–610. [https://doi.org/10.1016/1044-0305\(93\)85022-P](https://doi.org/10.1016/1044-0305(93)85022-P).
- [63] Lenke, H., Knackmuss, H.J., 1996. Initial hydrogenation and extensive reduction of substituted 2,4-dinitrophenols. *Appl Environ Microbiol* 62 (3), 784–790. <https://doi.org/10.1128/aem.62.3.784-790.1996>.
- [64] National Center for Biotechnology Information, 2024. [Translated] A kind of preparation method of 2-chloro-3-bromoaniline <https://pubchem.ncbi.nlm.nih.gov/patent/CN-113461538-A>.
- [65] Meijer, J., Lamoree, M., Hamers, T., Antignac, J.P., Hutinet, S., Debrauwer, L., et al., 2021. An annotation database for chemicals of emerging concern in exposome research. *Environ Int* 152. <https://doi.org/10.1016/j.envint.2021.106511>.
- [66] United States Environmental Protection Agency, 2024. 3-(2-chloroanilino)-3-oxopropanoic Acid - Chem Details <https://comptox.epa.gov/dashboard/chemical/details/DTXCID10314322>.
- [67] National Center for Biotechnology Information, 2024. Process for preparing 2-bromo-4,6-dinitroaniline. <https://pubchem.ncbi.nlm.nih.gov/patent/CS-759089-A3>.
- [68] Zhong, Y., Li, D., Mao, Z., Huang, W., Peng, P., Chen, P., et al., 2014. Kinetics of tetrabromobisphenol A (TBBPA) reactions with H₂SO₄, HNO₃ and HCl: Implication for hydrometallurgy of electronic wastes. *J Hazard Mater* 270, 196–201. <https://doi.org/10.1016/j.jhazmat.2014.01.032>.
- [69] Dehkordi, S.K., Paknejad, H., Blaha, L., Svecova, H., Grabic, R., Simek, Z., et al., 2022. Instrumental and bioanalytical assessment of pharmaceuticals and hormone-like compounds in a major drinking water source—wastewater receiving Zayandeh Rood river, Iran. *Environ Sci Pollut Res* 29 (6), 9023–9037. <https://doi.org/10.1007/s11356-021-15943-7>.
- [70] Nguyen, H.H., Ha, K.N., Huynh, D.L., Pham, D.D., Tran, T.M.D., Vo, V.G., et al., 2023. Secondary metabolites from leaves of bouea macrophylla. *Chem Nat Compd* 59 (3), 540–542. <https://doi.org/10.1007/s10600-023-04046-z>.
- [71] Gomez-Ruiz, B., Gómez-Lavín, S., Diban, N., Boiteux, V., Colin, A., Dauchy, X., et al., 2017. Efficient electrochemical degradation of poly- and perfluoroalkyl substances (PFASs) from the effluents of an industrial wastewater treatment plant. *Chem Eng J* 322, 196–204. <https://doi.org/10.1016/j.cej.2017.04.040>.
- [72] Schaefer, C.E., Choyke, S., Ferguson, P.L., Andaya, C., Burant, A., Maizel, A., et al., 2018. Electrochemical Transformations of Perfluoroalkyl Acid (PFAA) Precursors and PFAAs in Groundwater Impacted with Aqueous Film Forming Foams. *Environ Sci Technol* 52 (18), 10689–10697. <https://doi.org/10.1021/acs.est.8b02726>.
- [73] Corbet, A.S., 1935. The formation of hyponitrous acid as an intermediate compound in the biological or photochemical oxidation of ammonia to nitrous acid. *Biochem J* 29 (5), 1086–1096. <https://doi.org/10.1042/bj0291086>.
- [74] Scozzafava, A., Briganti, F., Supuran, C.T., 1998. Carbonic anhydrase inhibitors. Part V: inhibition of carbonic anhydrase isozymes I, II and IV with arsanilic acid derivatives. *Main Group Met Chem* 21 (6), 357–364.
- [75] Freeling, F., Scheurer, M., Sandholzer, A., Armbruster, E., Nödler, K., Schulz, M., et al., 2020. Under the radar – Exceptionally high environmental concentrations of the high production volume chemical sulfamic acid in the urban water cycle. *Water Res* 175. <https://doi.org/10.1016/j.watres.2020.115706>.
- [76] Propp, V.R., De Silva, A.O., Spencer, C., Brown, S.J., Catingan, S.D., Smith, J.E., et al., 2021. Organic contaminants of emerging concern in leachate of historic municipal landfills. *Environ Pollut* 276, 116474. <https://doi.org/10.1016/j.envpol.2021.116474>.
- [77] Liu, J., Mejia Avendaño, S., 2013. Microbial degradation of polyfluoroalkyl chemicals in the environment: a review. *Environ Int* 61, 98–114. <https://doi.org/10.1016/j.envint.2013.08.022>.
- [78] Liu, T., Hu, L.X., Han, Y., Xiao, S., Dong, L.L., Yang, Y.Y., et al., 2024. Non-target discovery and risk prediction of per- and polyfluoroalkyl substances (PFAS) and transformation products in wastewater treatment systems. *J Hazard Mater* 476 (March), 135081. <https://doi.org/10.1016/j.jhazmat.2024.135081>.
- [79] Shojaei, M., Kumar, N., Guelfo, J.L., 2022. An integrated approach for determination of total per- and polyfluoroalkyl substances (PFAS). *Environ Sci Technol* 56 (20), 14517–14527. <https://doi.org/10.1021/acs.est.2c05143>.
- [80] Sun, W., Zhang, P., Yang, B., Shu, J., Wang, Y., Li, Y., 2015. Products and mechanisms of the heterogeneous reaction of three suspended herbicide particles with NO₃ radicals. *Sci Total Environ* 514, 185–191. <https://doi.org/10.1016/j.scitotenv.2015.02.003>.
- [81] Jonkers, T.J.H., Meijer, J., Vlaanderen, J.J., Vermeulen, R.C.H., Houtman, C.J., Hamers, T., et al., 2022. High-performance data processing workflow incorporating effect-directed analysis for feature prioritization in suspect and nontarget screening. *Environ Sci Technol* 56 (3), 1639–1651. <https://doi.org/10.1021/acs.est.1c04168>.
- [82] Bond, T., Huang, J., Templeton, M.R., Graham, N., 2011. Occurrence and control of nitrogenous disinfection by-products in drinking water - A review. *Water Res* 45 (15), 4341–4354. <https://doi.org/10.1016/j.watres.2011.05.034>.